Comparison of Charge Transport and Opto-Electronic Properties of Pyrene and Anthracene Derivatives For OLED Applications

K. Uzun (✉ kubrauzun@ktu.edu.tr)

  Karadeniz Technical University: Karadeniz Teknik Universitesi   https://orcid.org/0000-0001-9751-0952

S. Sayın

  Giresun University: Giresun Universitesi

Ö. Tamer

  Sakarya University: Sakarya Universitesi

U. Çevik

  Karadeniz Technical University: Karadeniz Teknik Universitesi

---

Comparison of Charge Transport and Opto-Electronic Properties of Pyrene and Anthracene Derivatives For OLED Applications

K. Uzun[a], S.Sayın[b], Ö. Tamer[c], U.Çevik[a]

[a] *Department of Physics, Faculty of Sciences Karadeniz Technical University, 61080, Trabzon, Turkey*
[b] *Department of Environmental Engineering, Faculty of Engineering, Giresun University, 28200, Giresun, Turkey*
[c] *Department of Physics, Faculty of Arts and Sciences, Sakarya University, 54187, Sakarya, Turkey*
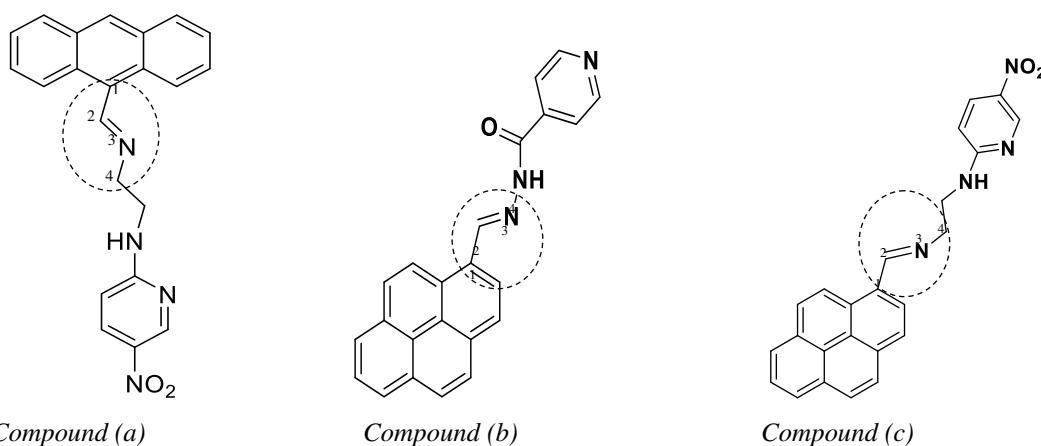
[*]Corresponding author: kubrauzun@ktu.edu.tr

ABSTRACT

In this paper, three organic semiconductors which are 9-[(5-nitropyridin-2-aminoethyl)iminiomethyl]-anthracene(**a**)and   *N'*-((pyren-4-yl)methylene)isonicotinohydrazide (**b**), and novel organic semiconductor *N*-(2-((pyren-4-yl)methyleneamino)ethyl)-5-nitropyridin-2-amine (**c**) have been prepared. Their structure have been assessed using NMR and elemental analysis techniques. While compound (a) and compound (c) have same wing unit ([(5-nitropyridin-2-aminoethyl) iminiomethyl]), compounds (b) and (c) have same core unit (5-nitropyridin-2-amine). Based upon TD-DFT and Marcus theories, we have explored the effect of molecular structure on the opto-electronic properties for OLED applications. Our results show that, wing units of molecules effects the opto-electronics properties a lot than core units. Such that, compounds (a) and (c) which have same wing unit, have been exhibited quite similar behaviours from points of both structural and opto-electronic parameters. Wheares, similar sitiation has not been observed for compounds (b) and (c) which have same core unit. More importantly accordingly our results, compounds (a) and (c) exhibit obvious advantages for organic electronic devices in terms of calculated opto-electronic and charge transport properties such as with better absorption and emission parameters, lower energy gaps and reorganization energies, higher charge mobility, etc.

Key words: DFT, reorganization energy, opto-electronic properties, pyrene, anthracene

1. Introduction

In 2000, Shirakawathe, MacDiarmid and Heeger [1] has awarded by Nobel Chemistry Prize for their discovery of some organic molecules showing semiconductor properties and this has attracted the interest of scientists in organic semiconductors and also revealed an area called "organic electronics" [2]. Organic electronic has an enormous potential for enlargement completing the range of classic semiconductor applications and for executing the applications that are difficult to do with traditional semiconconductors. In the past years, conjuge organic molecules have been broadly investigated and used in the organic electronic applications such us field effect transistor, solar cells and light emitting diode [3-5]. Optoelectronic properties of these devices associate with various factors, such as, electron density on the frontier molecular orbitals (FMOs), suitable charge carrier, the structural properties of molecules such us core unit or wing unit and the intermolecular interactions [6].

On the other hand, in recent years, many theoretical researchs have been investigated to predict and to relationship ensure organic materials characteristics. In consequence of energy gap of organic semiconductors can be predicted theoretically with the help of conjugation degree, optical and electronic properties of organic semiconductors materials can be adjustable as required and thus the design of new materials is easier and economical. Many studies have shown that the DFT and TD-DFT theories gives accurate results for π-conjugated systems abstract guzel]. Due to the wide p-electron system anthracene derivatives reach numerous applications in organic electronic devices such us thin-film transistors, solar cells, organic light emitting diodes (OLEDs) and Schottky diodes [7,8]. When Considered both intramolecular π-conjugation and powerfull intermolecular π- stacking of pyrene, pyrene derivatives could be proper for the structural requirements of organic semiconductors [9]. In this paper, a theoretical investigations about the effect of molecular structure on the vibrational, opto-electronic and charge transport properties of molecules based on anthracene and pyrene. Compound a (9-[(5-nitropyridin-2-aminoethyl) iminiomethyl]- anthracene) which has anthracene as central core and compound b (*N*-[2-((Pyren-4-yl)methyleneamino)ethyl-5-nitropyridin-2-amine) and compound c (*N'*-[((Pyren-4-yl)methylene) isonicotinohydrazide)) which have pyrene as central core which are shown in Scheme 1. While compound a and b have same wing group, compound b and c same core group. For this reason the effect of core and wing group thus electron donating, withdrawing and neutral groups on the opto-electronic and charge transport properties of molecules has been investigated and compared.

Compound (a)   *Compound (b)*   *Compound (c)*

Scheme 1. Chemical structures of compounds.

2. Materials and Computational Details

2.1. Synthesis

9-[(5-nitropyridin-2-aminoethyl)   iminiomethyl]-anthracene   (**a**)   and   *N'*-((pyren-4-yl)methylene)isonicotinohydrazide (**b**) were synthesized according to the literature procedures [S.F. Varol, S. Sayin, S. Eymur, Z. Merdan, D. Ünal. Org. Electron. 31, 25–30 (2016).; S. Sayin, S. F. Varol, Z. Merdan, S. Eymur. J Mater Sci: Mater Electron (2017) 28:13094–13100.]. The synthesis of *N*-(2-((pyren-4-yl)methyleneamino)ethyl)-5-nitropyridin-2-amine (**c**) was reported for the first time.

Synthesis of 9-[(5-nitropyridin-2-aminoethyl) iminiomethyl]-anthracene (a): Yield 85%, m.p.; 169-170°C. ^{1}H NMR (400 MHz, DMSO-d$_6$): δ 3.93 (brs, 2H, -C$\boldsymbol{H}_2$-NH), 4.14 (t, 2H, *J*=5.2 Hz, -C$\boldsymbol{H}_2$-N), 6.66 (d, 1H, *J*=8.8 Hz, Ar$\boldsymbol{H}$), 7.53 (p, 4H, *J*=8.0 Hz, Ar$\boldsymbol{H}$),8.12-8.15 (m, 3H, N$\boldsymbol{H}$ and Ar$\boldsymbol{H}$), 8.39 (brs, 1H, Ar$\boldsymbol{H}$), 8.51 (d, 2H, *J*=8.4 Hz, Ar$\boldsymbol{H}$), 8.70 (s, 1H, Ar$\boldsymbol{H}$), 8.98 (brs, 1H, Ar$\boldsymbol{H}$), 9.46 (s, 1H, -C$\boldsymbol{H}$=N) (see supporting information **Figure S1**). ^{13}C NMR (100 MHz, DMSO): δ42.17 (-$\boldsymbol{C}$H$_2$-NH), 61.26(-$\boldsymbol{C}$H$_2$-N), 125.45, 125.93, 127.15, 128.47, 129.20, 129.59, 129.77 and 131.24 (Ar$\boldsymbol{C}$), 134.81 (Ar$\boldsymbol{C}$-NO$_2$), 147.38 (Ar$\boldsymbol{C}$), 162.06 (-$\boldsymbol{C}$H=N), 162.26 (Ar$\boldsymbol{C}$-NH). Anal. Calcd. For C$_{22}$H$_{18}$N$_4$O$_2$ (%): C; 71.34, H; 4.90, N; 15.13. Found (%): C; 71.27, H; 5.83, N; 15.21.

Synthesis of N'-((pyren-4-yl)methylene)isonicotinohydrazide (b): Yield (210 mg, 72.1%); mp 263-265 °C. ^{1}H NMR (400 MHz DMSO-d$_6$): δ 7.92-7.93 (m, 2H, Ar$\boldsymbol{H}$), 8.14 (t, 1H, *J*=7.6 Hz, Ar$\boldsymbol{H}$), 8.27 (q, 2H, *J*=11.2 Hz, Ar$\boldsymbol{H}$), 8.38-8.41 (m, 4H, Ar$\boldsymbol{H}$), 8.60 (d, 1H, *J*= 8.0 Hz Ar$\boldsymbol{H}$), 8.82-8.86 (m, 3H, Ar$\boldsymbol{H}$), 9.53 (s, 1H, -C$\boldsymbol{H}$=N), 12.27 (s, 1H, N$\boldsymbol{H}$) (see supporting information **Figure S2**). ^{13}C NMR (100 MHz, DMSO): δ 122.02, 122.80, 124.16, 124.56, 125.70, 126.35, 126.68, 126.99, 127.10, 127.84, 129.05, 129.36, 130.55, 131.27, 132.62, 140.93, 148.33, 150.10, 150.90, 162.11 (**C**=O). Anal. Calcd. For C$_{23}$H$_{15}$N$_3$O (%): C; 79.07, H; 4.33, N; 12.03. Found (%): C; 79.14, H; 4.29, N; 11.97.

Synthesis of N-(2-((pyren-4-yl)methyleneamino)ethyl)-5-nitropyridin-2-amine (c): A flask was charged with 2-(2-aminoethylamino)-5-nitropyridine (151.9 mg, 0.834 mmol), 1-pyrenecarboxaldehyde (230.3 mg, 1.0 mmol) and 20 mL a mixture of THF/MeOH (1/1, v/v). The

reaction mixture was refluxed for 48 h. Then it was cooled to room temperature, and filtered. The crude was re-crystallized from EtOH, filtered and dried in an oven. Yield (200 mg, 50.8%); mp 167-168 °C . ^{1}H NMR (400 MHz DMSO-d$_6$): δ 3.87 (brs, 2H, -CH$_2$), 4.03 (t, 2H, J= 5.6 Hz, -CH$_2$), 6.66 (d, 1H, J=8.8 Hz, ArH), 8.13 (t, 2H, J=7.6 Hz, ArH), 8.21-8.38 (m, 7H, ArH), 8.55 (d, 1H, J=8.0 Hz, ArH), 8.97 (brs, 1H, -NH), 9.07 (d, 1H, J=9.6 Hz, ArH), 9.39 (s, 1H, -CH=N) (see Fig. 1). ^{13}C NMR (100 MHz, DMSO-d$_6$): δ 161.94, 147.32, 134.78, 132.74, 131.23, 130.55, 129.70, 129.03, 128.87, 127.83, 126.99, 126.94, 126.52, 126.22, 125.38, 124.44, 124.18, 123.49, 123.05, 60.70, 42.33. Anal. Calcd. For C$_{24}$H$_{18}$N$_4$O$_2$ (%): C; 73.08, H; 4.60, N; 14.20. Found (%): C; 73.13, H; 4.51, N; 14.09.

2.2. Computational Methods

All quantum chemical calculations interested in geometric parametres, opto-electronic and charge transport properties, vibrational wave numbers of the compounds have been carried out using the Gaussian 09w programme [12]. DFT/TD–DFT methods have been used to correlate structure-charge transport properties and understand to opto-electronic properties of these compounds. Hybrid functional of Beckethree–Lee–Yang–Parr (B3LYP) and (6-31+G(d,p)) basis set have been performed to optimized structure in ground and excited states and calculate HOMO, LUMO and energy gap [13,14]. The absorption and emission spectrums have been computed with TD-DFT-CAM-B3LYP [15]. The electronic transitions and oscillator strengths have been also calculated using the same method.

The rate of charge transfer K_{CT} which is extreme sensitive to structural parameters can be calculated according to Marcus theory with the following equation [16]:

$$K_{CT} = \frac{2\pi t^2}{\hbar} \sqrt{\frac{\pi}{\lambda k_B T}} \exp\left(-\frac{\lambda}{4 k_B T}\right) \qquad (1)$$

where T is the temperature, k$_B$ is the Boltzmann constant. The intra-molecular reorganization energy and intermolecular transfer integral are the major parameters for charge transfer properties of organic molecules [17]. λ is the reorganization energy that is the strengthor the electronphonon (vibration) and used to analyze charge transfer performance in the organic molecules. The reorganization energies have been calculated using Eq. (2) for hole and electron (λ_+ and λ_-) respectively.

$$\lambda_\pm = [E_\pm(g_0) - E_\pm(g_\pm)] + [E_0(g_\pm) - E_0(g_0)] \qquad (2)$$

Reorganization energy for hole (λ_+) represents the sum of the relaxation energy between the neutral back to cationic state and the relaxation energy between the cationic back to neutral state. The same for the reorganization energy of electron transport (λ_-) is equal to

the sum of the energies between neutral and anion state and the energy between anion back to neutral state [18,19].

On the other hand, we have been calculated the transfer integral with Koopmans's theorem. The transfer integral is strongly dependent on the charge and neutral molecules interactions and their geometries [20]. To evaluate the transfer integral the method is used to the half of the splitting of the HOMO and HOMO-1 or LUMO and LUMO+1 levels, for holes (t_h) or electrons (t_e) were calculated according to Eqs. (3) and (4), respectively:

$$t_h = \frac{E_{HOMO} - E_{HOMO-1}}{2} \qquad (3)$$

$$t_e = \frac{E_{LUMO+1} - E_{LUMO}}{2} \qquad (4)$$

To evaluate the oxidation and reduction ability of molecules, we have been calculated the ionization potential (IP) and electron affinity (EA) by the equations below.
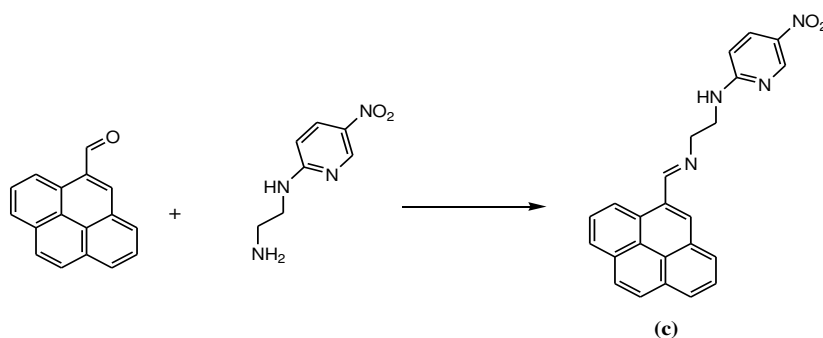
$$IP = E_+ - E_0 \qquad (5)$$

$$EA = E_0 - E_- \qquad (6)$$

3. Results and Discussions

3.1. Synthesis and Characterization of the Organic Semiconductors

9-[(5-nitropyridin-2-aminoethyl) iminiomethyl]-anthracene (**a**) and *N'*-((pyren-4-yl)methylene)isonicotinohydrazide (**b**) were synthesized according to the literature procedures [S.F. Varol, S. Sayin, S. Eymur, Z. Merdan, D. Ünal. Org. Electron. 31, 25–30 (2016).; S. Sayin, S. F. Varol, Z. Merdan, S. Eymur. J Mater Sci: Mater Electron (2017) 28:13094–13100.].
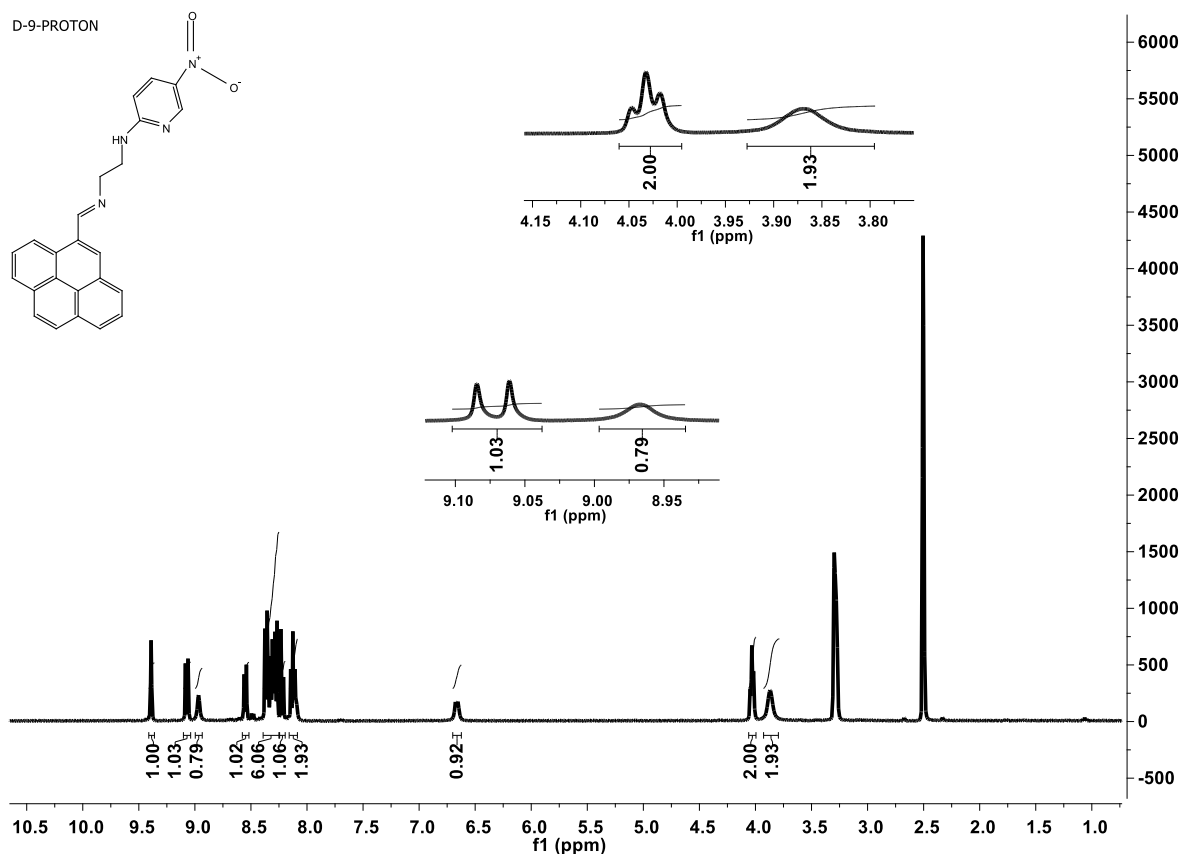

Scheme 2. Synthesis of *N*-(2-((pyren-4-yl)methyleneamino)ethyl)-5-nitropyridin-2-amine.

N-(2-((pyren-4-yl)methyleneamino)ethyl)-5-nitropyridin-2-amine (c) illustrated in Scheme 2 was synthesized in 50.8% yield for the first time by the reaction of 2-(2-aminoethylamine)-5-nitropiridine and 1-pyrenecarboxaldehyde in the presence of THF/MeOH. Structure of *N*-(2-((pyren-4-

yl)methyleneamino)ethyl)-5-nitropyridin-2-amine was assessed using ^{1}H-NMR and elemental analysis techniques.

NMR technique was used to confirm the structure of *N*-(2-((pyren-4-yl)methyleneamino)ethyl)-5-nitropyridin-2-amine. Figure 1 shows that compound **c** was successfully synthesized by appearing the proton of imine group at 9.39 ppm (1H) in the ^{1}H-NMR spectra (see Fig. 1).

Fig. 1. ^{1}H NMR (DMSO-d$_6$) spectra of *N*-(2-((pyren-4-yl)methyleneamino)ethyl)-5-nitropyridin-2-amine (c)
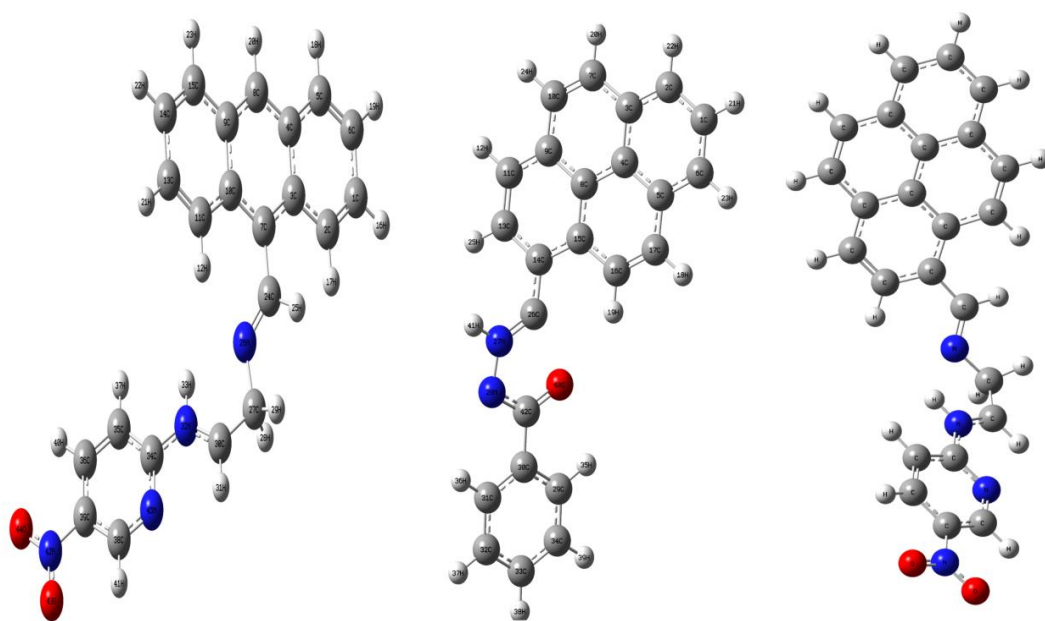
3.2. Molecular Design, Energy and Dipole Moment

The optimized structures of the ground state the studied compounds are shown in *Fig. 2*. The related parameters calculated for each compound with are listed in Table1. We can notice from Table 1 that, compound (a) has the shortest bond length meaning that compound (a) has the best charge transfer because the shorter length is an advantage for the intra-molecular charge transfer within the donor-acceptor type molecules [21].

Table 1. The DFT/B3LYP calculated total energy, dipole moment, bond lengths (Å) and dihedral angles (°) of the studied structures.
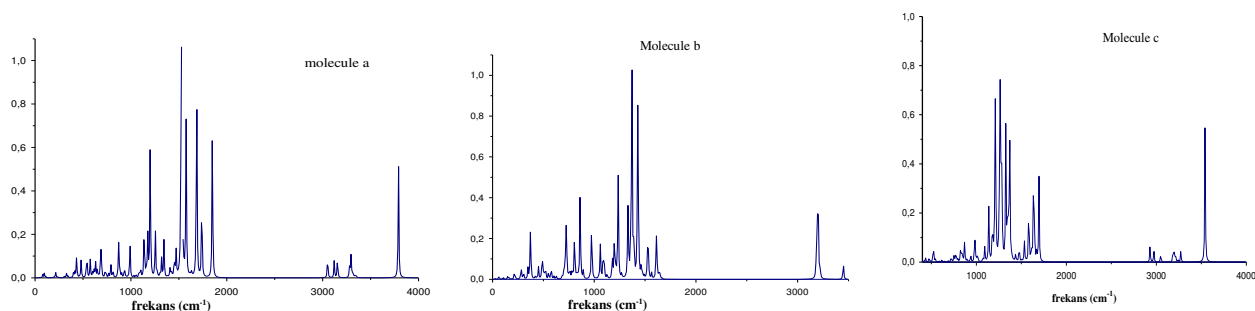
Molecule	Total Energy(Hartree)	Dipole Moment (Debye)	1-2	2-3	3-4	4-5	1-2-3-4	2-3-4-5
a	-1217,967	11,080	1,420	1,108	1,276	1,342	178,51	141,45
b	-1108,318	4,131	1,428	1,294	1,369	1,343	170,66	-1,836
c	-1294,219	12,172	1,467	1,282	1,456	1,498	175,33	132,90

The total moleculer energy has been used as a base criterion to validate a stable moleculer geometry. It can be seen that from the total energy values of the molecules, compound (c) has the best stable structure and in the second place is compound (a) which has same wing unit with compound (c). Thus we can say that, wing unit has plays an important role in the moleculer energy values and wing unit of compounds (a) and (c) make more stable the structure . In addition, while compounds (a) and (c) have similarly and big dihedral angle, compound (b) show growth tendency. These indicate that compound (a) and (c) have a good planarity aand thus they have better mobility of charges. In that, non-planar structures could reduce the intermoleculer interaction and affect the gap energy as we are going to realize in the next sections. We have calculated the vibrational frequencies due to ensure the stability of the optimized geometries and confirm that the lack of imaginary frequencies. The calculated IR spectra of the investigated compounds were showed in **Fig. 2**.

Fig. 2. Optimized structures of molecules a, b and c at the (B3LYP) and (6-31+G(d,p)).

We have calculated the vibrational frequencies due to ensure the stability of the optimized geometries and confirm that the lack of imaginary frequencies. The calculated IR
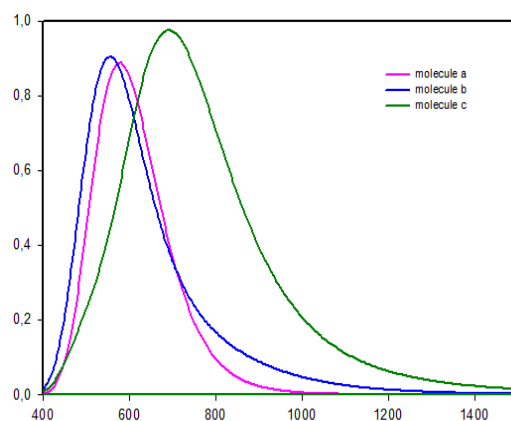
spectra of the investigated molecules were showed in **Fig. 3**. The strongest absorption band from IR spectrums have been observed at 1520,6 cm^{-1}, 1367,8 cm^{-1}, 1261,8 cm^{-1} for compounds (a),(b),(c) respectively, they correspond to C-N stretching vibrations. C=C, C=N, N=O strechings and N-H out of plane bending have been observed at double band range 1500-1800 cm^{-1}. The vibrations at 3524,6 cm^{-1}, 3796 cm^{-1} for compound (a), 3197,6 cm^{-1}, 3213,8 cm^{-1} for compound (b) and 3549 cm^{-1} , 3557,2 cm^{-1} for compound (c) correspond to C-H and O-H strecthings.

Fig.3. DFT calculated Infrared spectra of molecules by the use of B3LYP/6-31G(d) level of theory.

3.3. UV–vis spectral analysis

In order that reveal the molecular structure and opto-electronic properties relationships, the absorption spectra of molecules calculated with TD-DFT/CAMB3LYP method, 6-31G(d,p) basis sets. The UV-vis spectra of molecules are shown in **Fig. 4**. To further thought the optical properties and discover the nature of electronic transitions, the positions of absorption peaks and their assignment, the optical gap, the oscillator strengths (f), the light absorption efficiency (ηA), and the electronic dipole moments of molecules have been shown in **Table 2**.

Fig.4. Calculated absorption spectra for compounds at the TD-DFT/CAMB3LYP method, 6-31G(d,p).

The compounds (a),(b),(c) show maximum absorption wave lengths peaks at 581.2, 556, 691.2 nm, respectively. The dominant absorption bands are due to $\pi \to \pi^*$ electronic transitions and the maximum absorption wavelength corresponds to the excitation of an electron from HOMO to LUMO in all the compounds. In this respect, the studied compounds have broad absorption bands and red-shifts, causing the improved light harvesting ability. On the other hand, optical band gaps have been computed from onset of compounds absorption via the equation below [17], the optical band gabs are 1.66 eV, 1.58 eV, 1.18 eV for compounds (a),(b),(c) respectively.

$$E_g = \frac{1240}{\lambda_{onset}(nm)} \qquad (7)$$

On the other hand, we have also computed the light absorption efficiency $(\eta_A = 0.34, 0.30, 0.40$ for compounds a, b, c respectively, see Table2.$)$ that is essential parameter for the opto-electronic materials [27]:

$$\eta_A = 1 - 10^{-f} \qquad (8)$$

We can see from the light absorption efficiency values that, compound © has the best efficiency. This result has caused with the transition electronic dipole moments values of each compounds. In this respect, we can see from the our calculations that, the wing unit affectsextremely the optical parameters of organic semiconductors. Even though compound (c) shows a large absorption, the better optical parameters of compound (c) can be ascribed to better charge transfer properties as said prior. Thus we can say that compound (c) is more convenient from the point of absorption properties.

Table 2. The vertical excited energies and their oscillator strengths for the ground state (S0 → S1) of compounds calculations using TD-DFT/CAM-B3LYP.

Optical absorption properties of ground state (S0 → S1)						
Molecule	$\lambda_{abs}^{max}(nm)$	$E_g^{opt}(eV)$	Oscillator strength (f)	η_A	Transition	Electronic Dipole Moment
a	581.20	1.66	0.18	0.34	H→ L (98%)	2.73
b	556	1.58	0.15	0.30	H→ L (99%)	2.23
c	691.20	1.18	0.22	0.40	H→ L (98%)	2.77

3.4. Photoluminescence spectral analysis

The excited state geometries of compounds have been optimized using TD-B3LYP/6-311G(d,p) level of theory and from the optimized geometries, the emission spectra were calculated using the TD-DFT method at CAM-B3LYP/ 6-311G(d,p). The emission energies

and corresponding oscillator strength are summarized in Table 3. The calculated emission spectra for compounds are shown in **Fig. 5**. As is seen from Fig. 5., the moleculer structure has attention grabbing effect on photoluminescence process. The highest emission wavelength of the studied compounds are 636nm, 851 nm, 741nm for compounds (a),(b),(c), respectively. All the maximum emission peaks are assigned to $\pi\rightarrow\pi^*$ electronic transition arose from excited to the ground state (S_1 to S_0) and the emission spectra exhibit a red shifts for studied compounds. Among the studied compounds, the highest emission wavelength is observed in compound (b) with 851 nm, means that strong electron withdrawing with wing unit. All the above mentioned emission bands corresponds to the electronic transition between HOMO and LUMO.

On the other hand, the radiative lifetime τ (ns) which means the average time that molecules stay in their excited state before emitting photon of studied compounds have been calculated using Einstein transition probalities [28]:
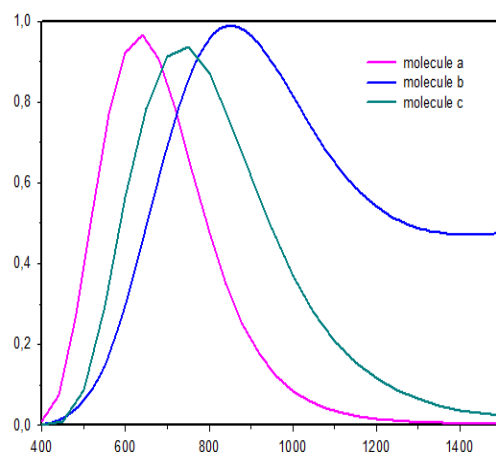
$$\tau = \frac{c^3}{2f(E_m)^2} \qquad\qquad (9)$$

where c is the velocity of light, E_{em} is the fluorescent energy, and f is the oscillator strength. The radiative life times have been found to be 24.32 ns, 77 ns, 38 ns for compounds a,b,c, respectively. Thus, we can say that, Compound a has shortest time in the excited state meaning that it has the best efficiency in the emission, secondly compound c has.

As to Stokes shift, we can notice that compounds (a) and (c) have quite similar behaviour again, compounds (a) and (c) showed considerable smaller Stokes shifts with 55nm and 50nm values. These results put forward small changing between ground and excited states and less energy loss along the relaxation process. We can say from the investigaions of emission properties that compounds (a) and (c) have similar parameters and they can be more suitable for OLED applications with same wing unit and the optical properties of the organic semiconductirs can be tuned with a more suitable wing unit.

Table 3. Emission parameters obtained by TD-DFT/CAM-B3LYP method for the compounds.

Optical emission properties (S1 → S0)						
Molecule	$\lambda_{emiss}^{max}(nm)$	$E_{em}(eV)$	Oscillator strength (f)	$\tau(ns)$	Transition	Stoke Shifts
a	636	1.83	0.28	24.32	L→ H (88%)	55
b	851	1.38	0.16	77	L→ H (80%)	295
c	741	1.62	0.23	38	L→ H (88%)	50

Fig.5. Calculated emission spectra for compounds at the TD-DFT/CAMB3LYP method, 6-31G(d,p).

3.5. Opto-Electronic Properties

3.5.1. Frontier Molecular Orbitals

As is known frontier orbital distributions can affect the charge transport properties and energy levels can be specified with electron giving a way ability of a core [22]. So, to better understand relation between the molecular structure and opto-electronic properties, we have investigated the charge density patterns of the frontier molecular orbitals: the highest occupied molecular orbitals (HOMO and HOMO-1) and the lowest unoccupied molecular orbitals (LUMO and LUMO+1) and their spatial distribution. The computed HOMOs, LUMOs and energy gaps (Eg) values of molecules at B3LYP/6-311G(d,p) have been given in the Table 4. These values match well with most work function of indium tin oxiede (ITO) electrode and suitable for exciton dissociation. As it can be seen, the HOMO energy levels of compounds (a) and (c) higher than compound (b). While, the LUMO energy levels of compounds (a) and (c) are lower than compound (b). This means that the injected electrons would be more stable for compounds (a) and (c). In addition we can say that for compound (b), the small HOMO energy level allows hole injection to efficiently reach the emitting layer. On the other hand, the energetic gap between HOMO and LUMO is higher in the compound (b) with Eg=3.0 eV and the lower value is associated to molecule c with E_g=1.86 eV. These results are in good agreement with the optical spectra which show a lower optical gap for compounds (a) and (c). Due to these results, we can say wing unit of compounds (a) and (c) could reduce E_g values. A profound understanding of frontier molecular orbital (FMO) of organic molecules is needful while adjustment the opto-electronic properties of the molecules. In the π conjugated molecules, the holes will migrate through HOMOs and electrons will migrate through the LUMOs of the nearby molecules. As it can be seen form Fig.6., the FMOs distribution.

HOMO and LUMO lobes are spread over the molecule only for compound (b). It shows the spatially lap over between the HOMO and LUMO is strong, thus stronger optical absorption can be observed for the transfer from HOMO to LUMO for compound (b). We can see also from the Fig.6. that the wing unit of an organic semiconductors has strong interaction with FMOs distribution. Because compound (a) and compound (c) have same wing unit as mentioned above and they have same FMOs behavior.

3.5.2. Charge Transport Properties

In this section, we have determined the key parameters of OLEDs which are ionization potential (IP), the electron affinity (EA) and reorganization energies (λ), binding energy, the chemical potential (η). These parameters which are very important to evaluate the energy barrier of holes and electron injection including charge mobility have been summarized in Table 4.
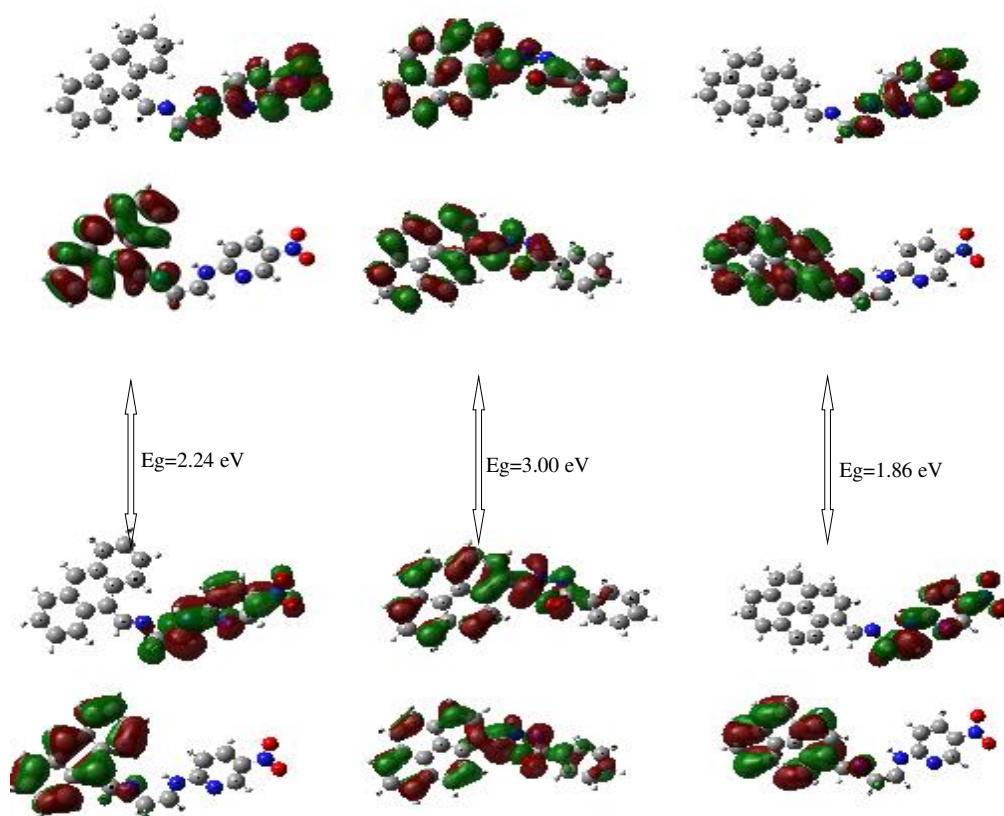
For ability of characterizing the reduction and oxidation, the IPs and EAs can be used. These properties also provide other useful informations about organic semiconductor devices [16]. Small IP values of emissive layer provide active hole transfer from the origin electrode. The IP values of compounds (a) and (c) have approximately same and higher than compound (b). Thus, we can say that molecule b is the best structure to create holes with lowest IP value 3.67 eV. It has been known that if molecules have high EA values, it displays a good electron accepting capacity [27]. Between studied molecules, compound (b) has biggest value of EA 2.85. Therefore, compound (b) could attain electrons from electrodes more easily than compounds (a) and (c).

Low reorganization energy for a better charge transfer and mobility, because K_{ET} is inverse ratio to reorganization values. Actually, the reorganization energy consist of nuclear reorganization energy and external polarized energy. But, because the external polarized energy is quite smaller compared to the nuclear reorganization energy [26], we only considered the nuclear part in this study. As it can be seen from Table 4, compounds (a) and (c) may be better for electron transport since they have electron transport reorganization energy λ_e lower than hole one λ_h. Similarly compound (b) faster hole transport than electron one λ_e. Thus, we can say that while compound (b) is a p-type organic semiconductors, compounds (a) and (c) are n-type organic semiconductors but all of them are suitable for charge transport applications because actually each one has low reorganization energy means higher charge transport rate. The binding energy is the energy difference among neutral exciton and free two electron-hole can be calculated with the energy difference among the electronic band gap and optical band

gap (the first singlet excitation energy). It is a very important factor for the electroluminescence materials [25]. The exciton binding energies (E_B) are 0.60 eV for compound (a) and 1.42 eV for compound (b), and 0.68 eV for compound (c), as shown in Table 4. This results indicate that excitons of molecules can be seperated easefully to free electrons and holes for all molecules due to quite low E_b values. But compounds (a) and (c) have exhibited similar behavior again and they have lower E_b values than compound (b). As is seen from Table 4, compounds (a) and (c) have better value both electron and hole intermolecular charge hopping ($K_{et}=6.1.10^{15}$, $K_h t= 0.86\ 10^{15}$ for compound (a), $K_{et} = 2.2.10^{15}$ $K_{ht}= 1.16\ 10^{15}$ for compound (c)) which approve the result found previously. Thus, we can emphasise that again compounds (a) and (c) exhibit same behavior in this respect also.

Table 4. DFT/B3LYP/(6-311G(d,p)) calculated electronic and charge transport parameters of studied molecules.

Electronic Parameters	Molecule a	Molecule b	Molecule c
E_{HOMO}	-4.89	-5.39	-4.52
E_{LUMO}	-2.65	-2.39	-2.66
E_g	2.24	3.00	1.86
E_{HOMO-1}	-5.76	-5.66	-6.08
E_{LUMO+1}	-2.15	-2.38	-2.25
λ_e	0.15	0.23	0.22
λ_h	0.21	0.18	0.26
EA	1.47	2.85	1.63
IP	6.22	3.67	6.06
η	2.37	0.42	2.21
t_h	0.44	0.13	0.43
t_e	0.25	0,05	0.20
E_b	0.60	1.42	0.68
K_{et}	$6.1.10^{15}$	$9.8.\ 10^{12}$	$2.2.10^{15}$
K_{ht}	$0.86\ 10^{15}$	$4.1.\ 10^{13}$	$1.16\ 10^{15}$

Figure 6. The ground state density plot of the FMOs of compound *a* and compound *b* and their ionic forms calculated at the B3LYP7/(6-311++G(d,p)) level of theory in the gas phase.

4. Conclusion

Theoretical calculations, allowed us to assess the role of the wing unit and core unit of the organic molecules on the optoelectronic properties of these materials. The fundamental parameters involved in structural, vibrational, charge transport and opto-electronic properties of pyrene and anthracene derivatives were analyzed using quantum chemical methods. The calculated optical properties show that, compounds (a) and (c), which have same wing units, indicate better absorption and emission properties compared to compound (b). The analysis of frontier molecular orbitals observed that depending on the molecular strucure, compounds (a) and (c) have same FMOs distribution and they have lower energy gaps values than compound (b). Thus we can say that, the wing unit of an organic semiconductors has strong interaction with FMOs distribution of molecules. We see from calculated charge transport properties that while compound (b) is a p-type semiconductor, compounds (a) and (c) are n–type semiconductors. But all three compounds have efficient electron and hole transport with quite high intermolecular charge hopping rates. The binding energies of compounds are quite low for all three compounds, so we can say, excitons of these compounds can be separated easily to free electrons and holes. This result is also an advantage for opto-electronic applications. All

these interesting optoelectronic and charge transport properties make all three studied compounds a potential candidate for optoelectronic devices especially OLED application. But compounds (a) and (c) exhibit obvious advantages for organic electronic devices in terms of mentioned properties such as with better absorption and emission parameters, lower energy gaps and reorganization energies, higher charge mobility, etc. On the other hand, we should emphasised that, wing units of molecules effects the opto-electronics and charge transport properties a lot than core units. Such that, compounds (a) and (c) which have same wing unit, have been exhibited quite similar behaviours from points of both structural and opto-electronic and charge transport properties. Wheares, similar situation has not been observed for compounds (b) and (c) which have same core unit. Thus, we can say, wing units plays a key role in the charge transport and opto-electronic properties. We hope that our study could provide some clues for the experimentalists to desingn and synthesize new organic semiconductors to gaion a better understanding of the moleculer structures effect on the oopto-electronic and charge transport properties.

Conflicts of interest/Competing interests :

- The authors have no relevant financial or non-financial interests to disclose.
- The authors have no conflicts of interest to declare that are relevant to the content of this article.

Availability of data and material:

All data generated or analysed during this study are included in this published article [and its supplementary information files].

Code availability:

The codes generated during the current study are available from the corresponding author on reasonable request.

Authors' contributions:

All authors contributed to the study conception and design. Material preparation, data collection and analysis were performed by Kübra Uzun, Serkan Sayın. The first draft of the manuscript was written by Kübra Uzun and all of the authors commented on previous versions of the manuscript. All authors read and approved the final manuscript.

References

[1] Shirakawa H., Louis E. J. MacDiarmid A. G., Chiang C. K., and Heeger A. J., Synthesis of electrically conducting organic polymers: halogen derivatives of polyacetylene, $(CH)_x$,J. Chem. Soc. Chem. Commun. (1977). 578-579.

[2] S.C. Rasmussen, Electrically Conducting Plastics: Revising the History of Conjugated Organic Polymers, American Chemical Society, 10, (2011) 147-163.

[3] A. Ahmad, Organic semiconductors for device applications: current trends and future prospects, J Polym Eng, 34, (2014) 279–338.

[4] R. N. K. Senthilkumar, Charge transport and optical properties of cross-conjugated organic molecules: A theoretical study, Org. Electron., 15 (2014) 1607–1623.

[5] X. Guo, N. Zhou, S.J. Lou, J. Smith, D.B. Tice, J.W. Hennek, R.P. Ortiz, J.T.L. Navarrete, S. Li, J. Strzalka, L.X. Chen, R.P.H. Chang, A. Facchetti, T.J. Marks, Polymer solar cells with enhanced fill factors, Nat. Photon, 7 (2013) 825–833.

[6] **S.Ahmed** and **D.J. Kalita**, Charge transport in isoindigo-dithiophenepyrrole based D-A type oligomers: A DFT/TD-DFT study for the fabrication of fullerene-free organic solar cells, J. Chem. Phys, 149 (2018) 234906-234917.

[7] A.V. Kukhta, I.N. Kukhta, N.A.Kukhta, O.L.Neyra, and E. Meza, DFT study of the electronic structure of anthracene derivatives in their neutral, anion and cation forms, Journal of Physics B, 41 (2007)1-7.

[8] J.P. Perdew, J.A. Chevary, S.H. Vosko, K.A. Jackson, M.R. Pederson, D.J.Singh, C. Fiolhais, Atoms, molecules, solids, and surfaces: applications of the generalized gradient approximation for exchange and correlation, Phys Rev B, (1992) 46 6671–6687.

[9] G.V. Baryshnikov, B. F. Minaev, M.l. Pittelkow, C.B. Nielsen , R. Salcedo, Nucleus-independent chemical shift criterion for aromaticity in π-extended tetraoxa[8]circulenes, Journal of Molecular Modeling, **19**, (2013) 847–850.

[10] S.F. Varol, S. Sayin, S. Eymur, Z. Merdan, D. Ünal. Synthesis of isoniazid substituted pyrene (PINHy), and investigation of its optical and electrochemical features as tunable/flexible OLEDs, Org. Electron. 31, (2016) 25–30

[11] S.Sayin, S.F. Varol, Z. Merdan, S. Eymur, Synthesis of isoniazid substituted pyrene (PINHy), and investigation of its optical and electrochemical features as tunable/flexible OLEDs, Journal of Materials Science Materials in Electronics, 17 (2017) 13094-13100.

[12] T. Yanai, D.P.Tew, N.C.Handy, A new hybrid exchange-correlation functional using the Coulomb-Attenuating Method (CAM-B3LYP), Chemical Physics Letters 393 2004 51-57.

[13] R.A. Marcus, N. Sutin, Electron transfers in chemistry and biology, Biochim. Biophys. Acta Rev. Bioenergy 811 (1985) 265–322.

[14] K.V. Mikkelsen, M.A. Ratner, Electron tunneling in solid-state electron-transfer reactions, Chem. Rev. 87 (1987) 113–153.

[15] H.L. Tavernier, M.D. Fayer, Distance dependence of electron transferin DNA: the role of the reorganization energy and free energy, J.Phys. Chem. B 104 (2000) 11541–11550.

[16] R. Nithya, M. Sowmiya, P. Kolandaivel, K. Senthilkumar, Structural, optical, and charge transport properties of cyclopentadithiophene derivatives: a theoretical study, Struct Chem. 25 (2014), 715-731.

[17] R. Chouk, M. Bergaoui, N. Jaballah, M. Majdoub, M. Khalfaoui, Shedding light on structural, optoelectronic and charge transport properties of PPV stereoisomers for multilayer OLED application: A first principle computational studies, Journal of Molecular Liquids 284 (2019) 193–202.

 [18] B.C. Lin, C.P. Cheng, Z.P.M. Lao, Reorganization energies in the transports of holes and electrons in organic amines in organic electroluminescence studied by density functional theory, J. Phys. Chem. A107 (2003) 5241.

 [19] H. Ma, N. Liu, J.-D. Huang, A DFT study on the electronic structures and conducting properties of Rubrene and its derivatives in organic field-effect transistors, Sci. Rep. 7 (2017).

[20] J. C. S.García and A. J. P. Jiménez, Theoretical study of stability and charge-transport properties of coronene molecule and some of its halogenated derivatives: A path to ambipolar organic-based materials, The J. of Chem. Phys. 141 (2014) 134708-134716.

[21] A. Hlel, A. Mabrouk, M. Chemek, I. Ben Khalifa, K. Alimi, A DFT study of charge transfer and opto-electronic properties of some new materials involving carbazole units, Comp. Cond. Matter. 3 (2015) 30-40.

[22] N. Wazzan, Reda. M. El-Shishtawy, A. Irfan, DFT and TD–DFT calculations of the electronic structures and photophysical properties of newly designed pyrene-core arylamine derivatives as hole-transporting materials for perovskite solar cells, Theoretical Chemistry Accounts. 137 (2018) 1-15.

[23] M. Ottonelli, M. Piccardo, D. Duce, S. Thea, G. Dellepiane, Koopmans' Transfer integral calculation: a comparison between the Hartree-Fock and the Density Functional results, Energy Procedia 31 (2012) 31 – 37.

[24] L. Zhang, W. Shen, R. He, X. Liu, X. Tang, Y. Yang, M. Li, Fine structural tuning of diketopyrrolopyrrole-cored donor materials for small molecule-fullerene organic solar cells: a theoretical study, Org. Electron. 32 (2016) 134.

[25] Z.Z. Suna, Y.L.Xua, R.Zhub, H.Y.Liuc, How to stabilize the HOMO levels and to improve the charge transport properties of hole-transporting materials? Probing the effects of molecular symmetry, Org.Electron. 63 (2018) 86–92.

[26] J.E. Norton, J.L. Brédas, Polarization Energies in Oligoacene Semiconductor Crystals J. Am. Chem. Soc. 130 (2008) 12377–12384.

[27] H.S. Nalwa, Handbook of Advanced Electronic and Photonic Materials and Devices: Semiconductors, Academic Press, 1 (2001) 313-316.

[28] J.K. Rice, L. Pasternack, H. Nelson, Einstein transition probabilities for the AlH a 1Π-X 1Σ+ transition, Chem. Phys. Lett. 43 (1992) 189-196.
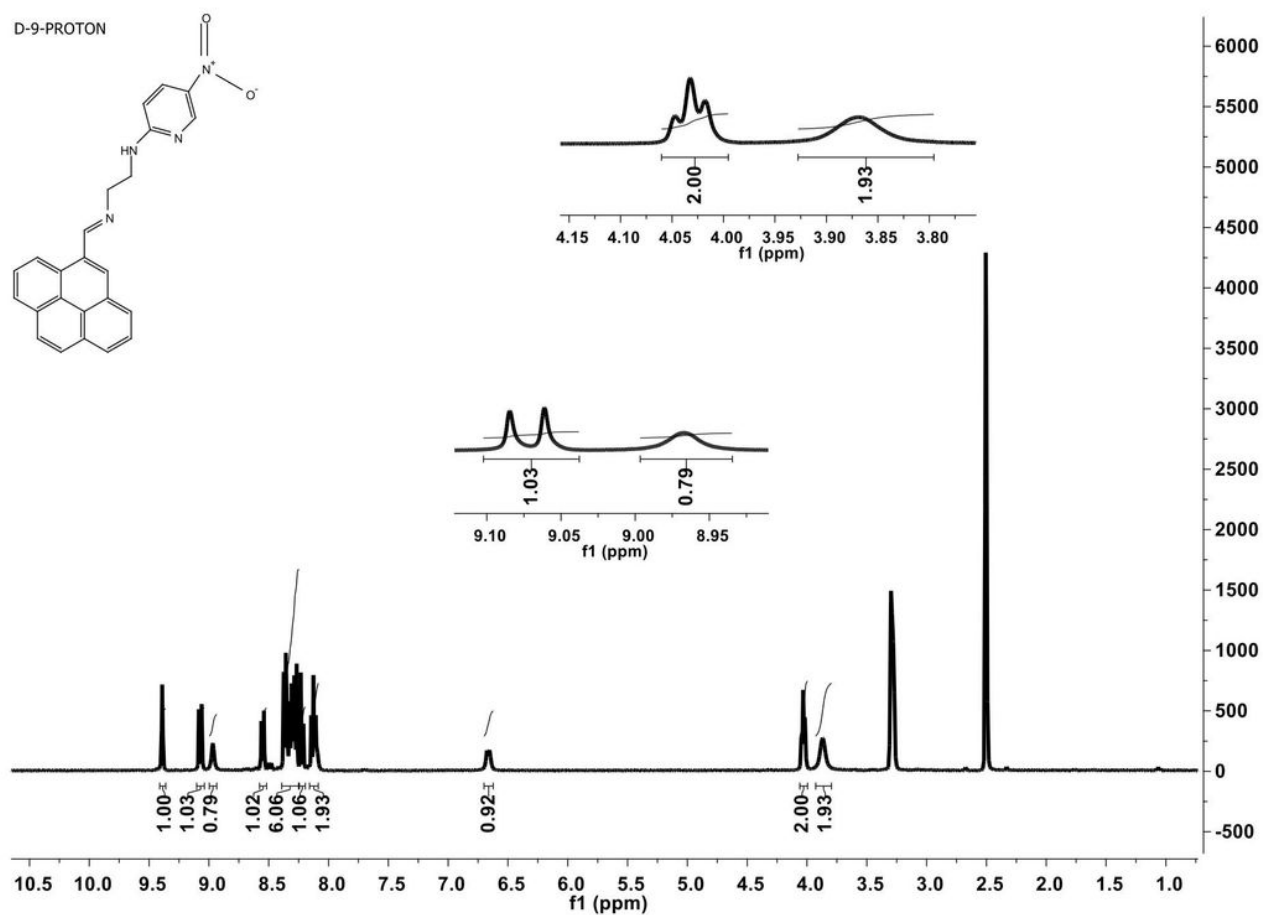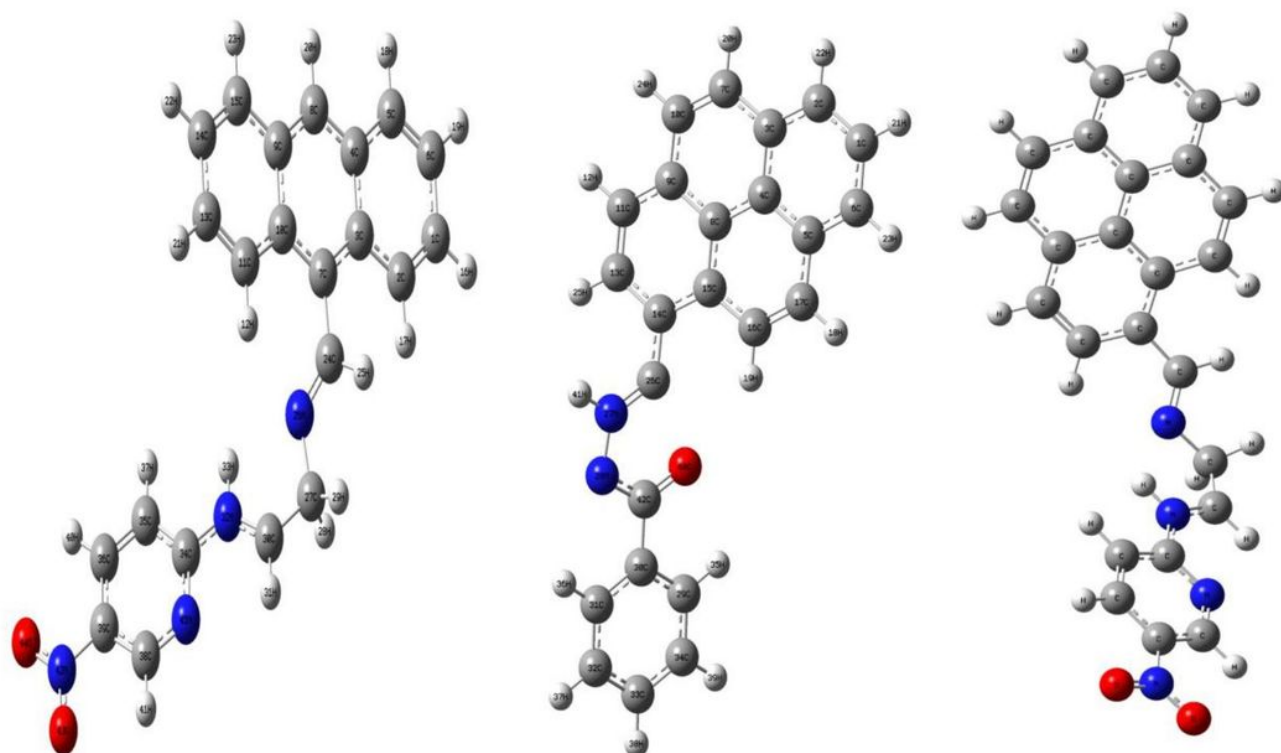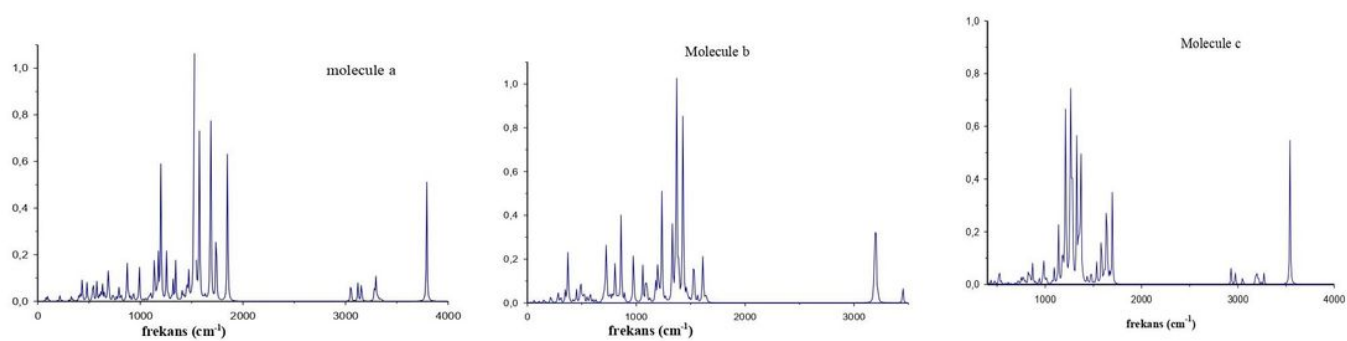
Figures

Figure 1

1H NMR (DMSO-d6) spectra of N-(2-((pyren-4-yl)methyleneamino)ethyl)-5-nitropyridin-2-amine (c)
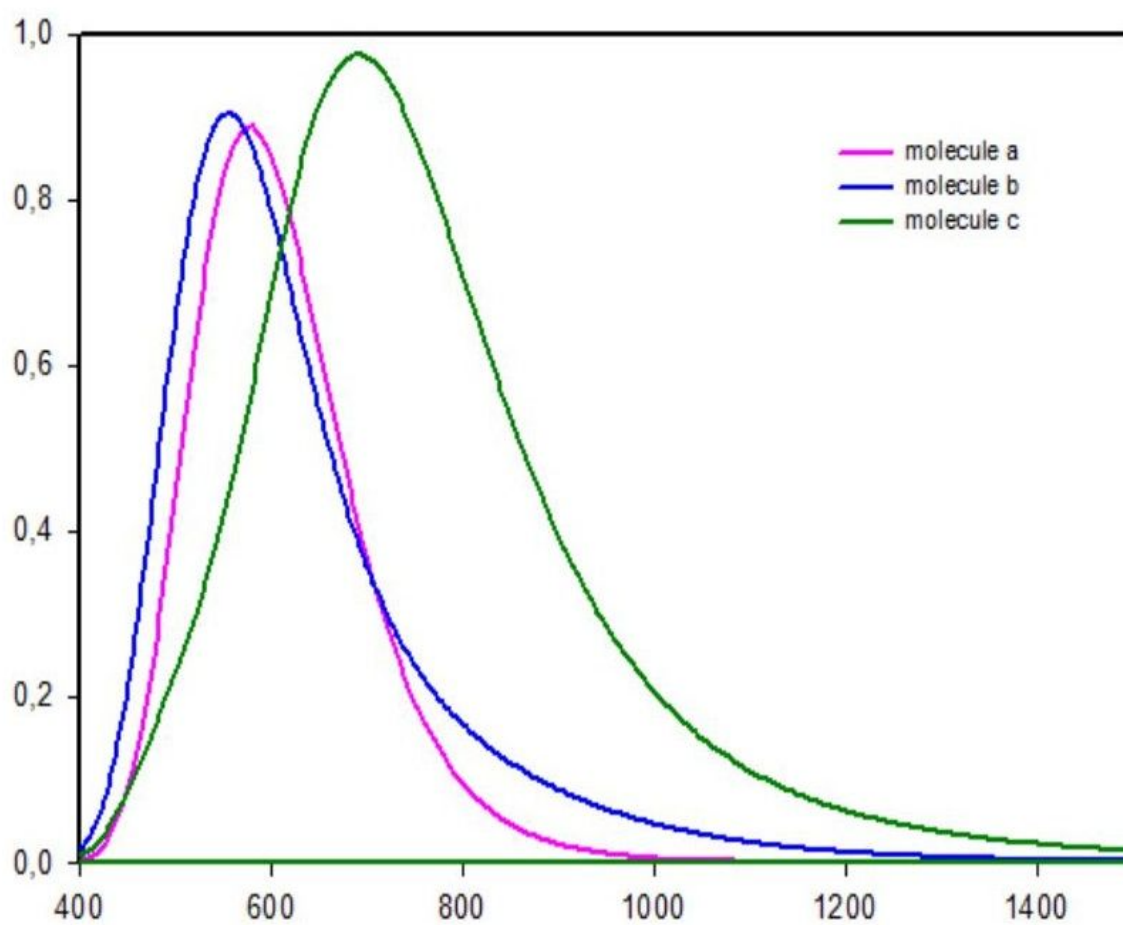
Figure 2

Optimized structures of molecules a, b and c at the (B3LYP) and (6-31+G(d,p)).
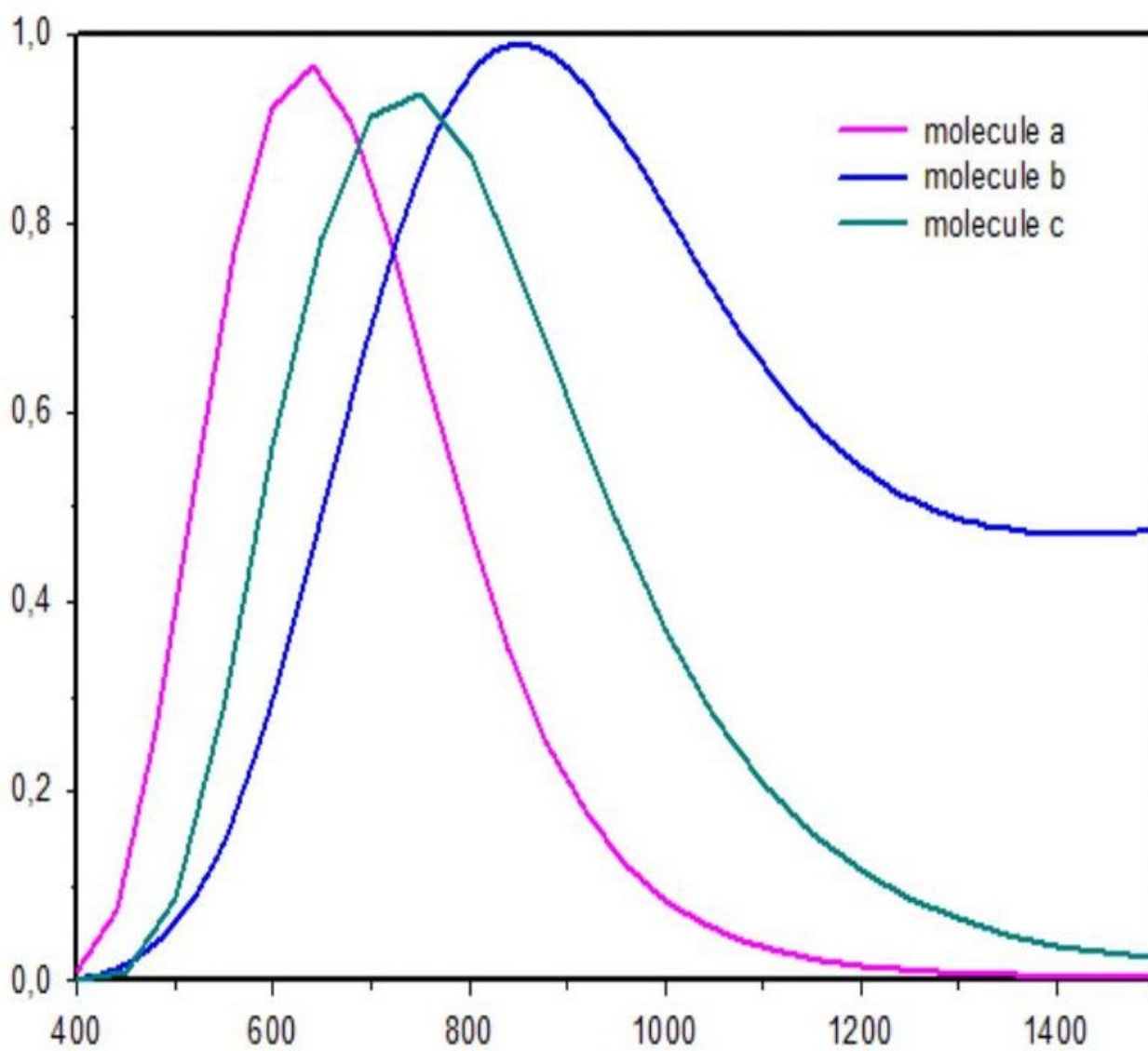

Figure 3

DFT calculated Infrared spectra of molecules by the use of B3LYP/6-31G(d) level of theory.
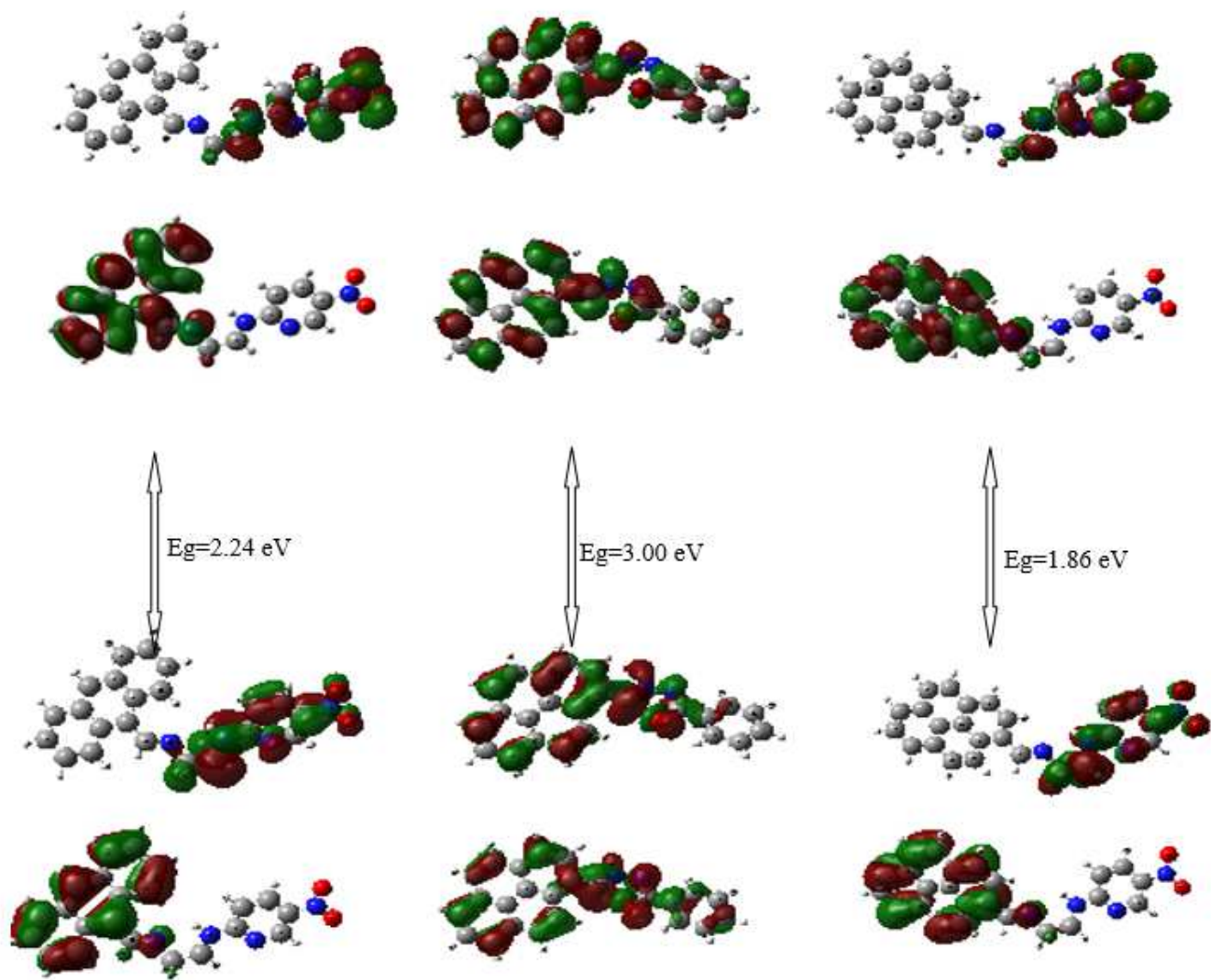
Figure 4

Calculated absorption spectra for compounds at the TD-DFT/CAMB3LYP method, 6-31G(d,p).
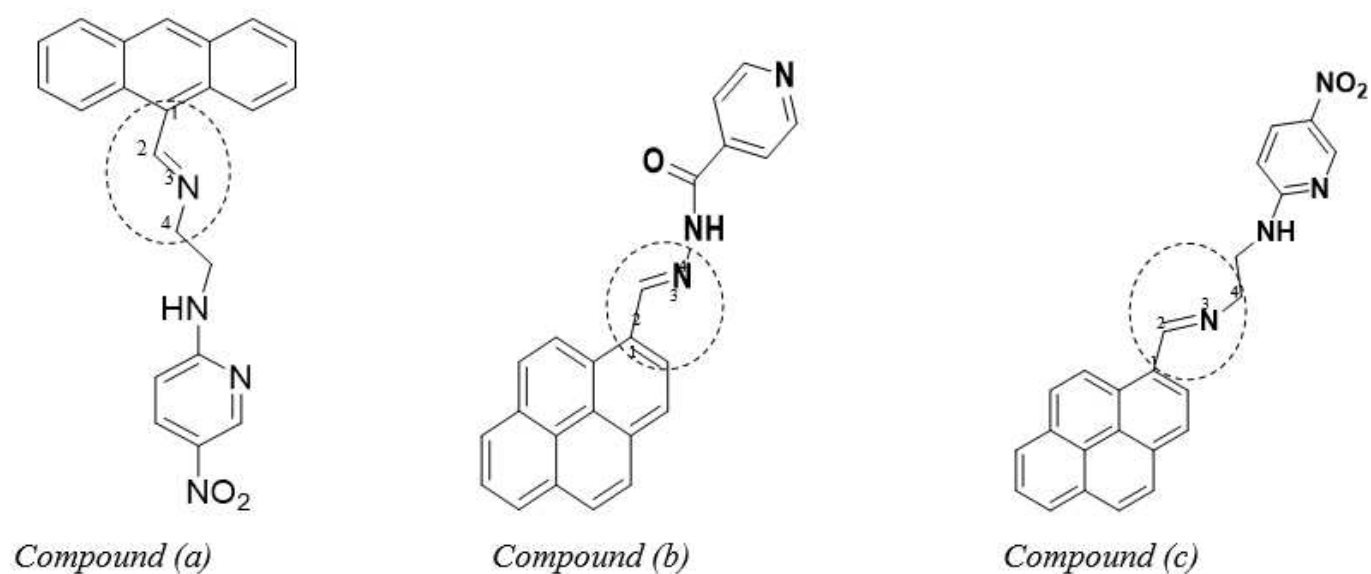
Figure 5

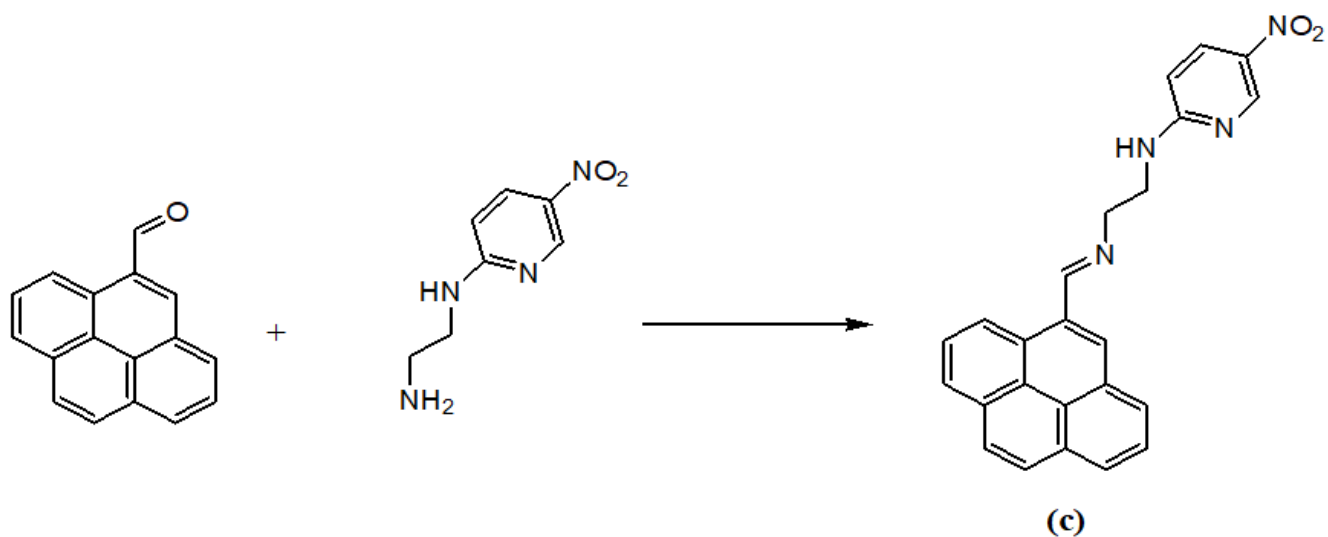Calculated emission spectra for compounds at the TD-DFT/CAMB3LYP method, 6-31G(d,p).

Figure 6

The ground state density plot of the FMOs of compound a and compound b and their ionic forms calculated at the B3LYP7/(6-311++G(d,p)) level of theory in the gas phase.

Compound (a)   Compound (b)   Compound (c)

Figure 7

Scheme 1. Chemical structures of compounds.

(c)

Figure 8

Scheme 2. Synthesis of N-(2-((pyren-4-yl)methyleneamino)ethyl)-5-nitropyridin-2-amine.

Supplementary Files

This is a list of supplementary files associated with this preprint. Click to download.

- supportinginfo.docx